



Contents lists available at ScienceDirect

## Spectrochimica Acta Part A: Molecular and Biomolecular Spectroscopy

journal homepage: [www.elsevier.com/locate/saa](http://www.elsevier.com/locate/saa)

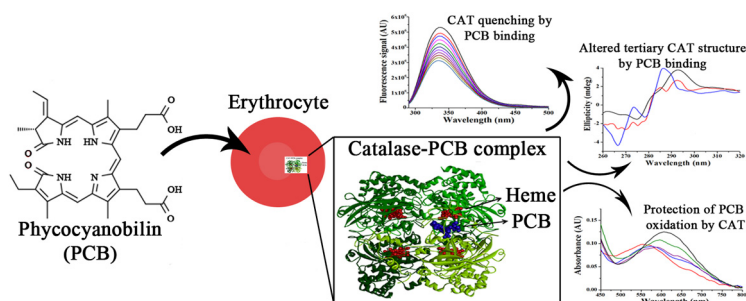
## Nutraceutical phycocyanobilin binding to catalase protects the pigment from oxidation without affecting catalytic activity

Nikola Gligorijević<sup>a</sup>, Simeon Minić<sup>b</sup>, Milica Radibratović<sup>c</sup>, Vassiliki Papadimitriou<sup>d</sup>, Olga Nedić<sup>a</sup>, Theodore G. Sotiroudis<sup>d</sup>, Milan R. Nikolić<sup>b,\*</sup><sup>a</sup> INEP Institute for Application of Nuclear Energy, University of Belgrade, Belgrade-Zemun, Serbia<sup>b</sup> Department of Biochemistry & Center of Excellence for Molecular Food Sciences, University of Belgrade – Faculty of Chemistry, Belgrade, Serbia<sup>c</sup> Department of Chemistry, Institute of Chemistry, Technology and Metallurgy, University of Belgrade, Belgrade, Serbia<sup>d</sup> National Hellenic Research Foundation, Institute of Chemical Biology, Athens, Greece

## HIGHLIGHTS

- Catalase binds nutraceutical phycocyanobilin.
- Binding changes tertiary enzyme structure, without affecting its activity.
- Binding protects the pigment from radical-induced oxidation.
- Results imply pigment's prolonged half-life and bioactivity *in vivo*.

## GRAPHICAL ABSTRACT



## ARTICLE INFO

## Article history:

Received 28 September 2020

Received in revised form 2 January 2021

Accepted 9 January 2021

Available online 18 January 2021

## Keywords:

Phycocyanobilin

Catalase

Binding

Structure

Activity

## ABSTRACT

Phycocyanobilin is a dark blue linear tetrapyrrole chromophore covalently attached to protein subunits of phycobiliproteins present in the light-harvesting complexes of the cyanobacteria *Arthrospira platensis* (Spirulina “superfood”). It shows exceptional health-promoting properties and emerging use in various fields of bioscience and industry. This study aims to examine the mutual impact of phycocyanobilin interactions with catalase, a life-essential antioxidant enzyme. Fluorescence quenching experiments demonstrated moderate binding ( $K_a$  of  $3.9 \times 10^4 \text{ M}^{-1}$  at  $25^\circ\text{C}$ ;  $n = 0.89$ ) (static type), while van't Hoff plot points to an enthalpically driven ligand binding ( $\Delta G = -28.2 \text{ kJ mol}^{-1}$ ;  $\Delta H = -41.9 \text{ kJ mol}^{-1}$ ). No significant changes in protein secondary structures ( $\alpha$ -helix content  $\sim 22\%$ ) and thermal protein stability in terms of enzyme tetramer subunits ( $T_m \sim 64^\circ\text{C}$ ) were detected upon ligand binding. Alterations in the tertiary catalase structure were found without adverse effects on enzyme activity ( $\sim 2 \times 10^6 \text{ IU/mL}$ ). The docking study results indicated that the ligand most likely binds to amino acid residues (Asn141, Arg 362, Tyr369 and Asn384) near the cavity between the enzyme homotetramer subunits not related to the active site. Finally, complex formation protects the pigment from free-radical induced oxidation (bleaching), suggesting possible prolongation of its half-life and bioactivity *in vivo* if bound to catalase.

© 2021 Elsevier B.V. All rights reserved.

## 1. Introduction

Phycobiliproteins are deep-coloured, fluorescent water-soluble proteins mainly present in cyanobacteria (blue-green algae) and Rhodophyta (red algae) [1]. Their function is to harvest light,

\* Corresponding author.

E-mail address: [mnikolic@chem.bg.ac.rs](mailto:mnikolic@chem.bg.ac.rs) (M.R. Nikolić).

enabling photosynthesis and other biological processes [2]. The blue colour of *Arthrospira platensis* (commonly called Spirulina) main biliprotein C-phycoerythrin (C-PC) originates from the phycoerythrin (PCB) chromophore. It is an open-chain tetrapyrrole structure covalently attached to protein subunits via thioether bonds [1]. Many pigments in living systems contain similar open tetrapyrrole molecules, such as bilirubin and biliverdin in vertebrates [2]. C-Phycocyanin has many potential applications. Its usage as a food additive and colourant has already been well-established [3]. To date, studies have shown that C-PC has potent antioxidant and anti-tumour activity. Its role in inflammation and enhancement of immune response has also been described [1,4,5]. One of the essential phycobiliprotein applications is their use as fluorescent markers in biomedical research [6]. Positive C-PC health effects are primarily derived from PCB [7–10].

Catalase is an enzyme involved in defence mechanisms against oxidative damage, and it converts hydrogen peroxide ( $H_2O_2$ ) to oxygen and water. Hydrogen peroxide is toxic due to its ability to form reactive oxygen species and participates in the Fenton reaction. This molecule can also act as a second messenger in many biological processes such as apoptosis, changes in morphology and cell proliferation [11]. Typical catalases are homotetramers with molecular masses ranging from 200 to 350 kDa. Each subunit of an animal and human catalase is 62 kDa, heme *b* as a prosthetic group and NADPH as a cofactor [12]. In humans, catalase is expressed in every organ, and the highest levels are found in the liver, kidneys and erythrocytes. In erythrocytes, where high production of  $H_2O_2$  occurs, catalase is responsible for more than 50% of its turnover [12]. So far, binding of many small bioactive molecules to catalase has been characterised. Some of these molecules are potent antioxidants, including vitamin C [13], resveratrol [14], curcumin [15] and quercetin [16]. They are capable of influencing both the structure and the activity of this enzyme.

Both covalent (with  $\beta$ -lactoglobulin) and non-covalent (with human or bovine serum albumin) interactions of PCB with various proteins have already been described [17–19]. Due to these interactions, the properties of these proteins are changed, including protein structure, increased stability and higher oxidation resistance. Protection from oxidation appears to be mutual, as binding proteins were shown to protect PCB from oxidation, thus prolonging its antioxidant activity [18,19]. Since both catalase and PCB are involved in antioxidant protection, it seemed reasonable to investigate in detail their potential interaction and its possible beneficial physiologic effects. The primary purpose of this study was to examine the binding capacity of catalase to PCB. Further, we explored the consequences of interactions on both the enzyme (possible alterations of its structure and activity) and the pigment (protection from free-radicals induced oxidation).

## 2. Materials and methods

### 2.1. Materials

All chemicals used were purchased from Sigma (Germany) and were of analytical grade or higher. Isolation, purification and PCB characterisation were performed using commercial Hawaiian Spirulina Pacifica powder (Nutrex, USA) and a previously described protocol [20]. Stock solutions of PCB were prepared by dissolving dried pigment in HPLC grade methanol (for circular dichroism studies) or anhydrous DMSO (for all other experiments). The concentration of PCB was determined by diluting aliquots in HCl/MeOH (1:19; v/v), measuring absorbance at 680 nm and using the extinction coefficient of  $37900\text{ M}^{-1}\text{ cm}^{-1}$  [21]. Bovine liver catalase powder (Product No. C-9322; 2000–5000 units/mg protein, molecular weight 250 kDa) was purchased from Sigma. It dis-

solved in 20 mM phosphate buffer, pH 7.4, and dialysed overnight in the same buffer. The next day, the catalase solution was centrifuged at 12,000g for 1 min at room temperature and the resulting supernatant was used for all experiments. The catalase concentration was determined by measuring absorbance at 276 nm using an extinction coefficient of  $\epsilon_{1\%}^{1\text{cm}}=12.9$  [22]. All solutions were prepared with ultra-pure water and the final concentration of organic solvents did not exceed 1% in any experiment. All experiments were performed in triplicate in the same phosphate buffer. All experimental results reported were based on averaging results of repeated triplicates, with the SD not exceeding 5% of the reported average.

### 2.2. Spectrofluorimetric analysis of catalase/phycoerythrin complex formation

All fluorescence spectra were recorded on a FluoroMax-4 spectrofluorometer (Horiba Scientific, Japan), equipped with a Peltier temperature controller unit connected with a cuvette holder. 3.5 mL quartz cuvettes were used, with a 2 mL total volume of reaction.

Determination of a binding constant between catalase and PCB was performed by titrating the enzyme with increasing pigment concentrations and recording fluorescence emission spectra. The catalase concentration was  $0.5\ \mu\text{M}$ , and PCB was added in a concentration range from  $0.5$  to  $5\ \mu\text{M}$ . The enzyme was excited at 280 nm, an excitation wavelength for both Trp and Tyr residues, and emission spectra were recorded from 290 to 500 nm. Excitation and emission slit widths were set to 5 nm. Control spectra obtained for each tested PCB concentration were subtracted from the appropriate spectra obtained in the presence of both catalase and PCB. The change in catalase emission intensity maximum at 339 nm was used to determine the affinity constant ( $K_a$ ). The resulting fluorescence intensity was first corrected for the inner filter effect of PCB using a common equation:

$$F_c = F_0 \times 10^{(A_{ex} + A_{em})/2}$$

where  $F_c$  is a corrected fluorescence intensity,  $F_0$  is a measured fluorescence and  $A_{ex}$  and  $A_{em}$  are absorbances at wavelengths of excitation and emission, respectively.

The quenching type was determined by preparing a Stern-Volmer (SV) plot and calculating the SV quenching constant ( $K_{SV}$ ) using the following equation [23]:

$$\frac{F_0}{F} = 1 + k_q \tau_0 [Q] = 1 + K_{SV} [Q]$$

where  $F_0$  and  $F$  are emission intensities without and in the presence of PCB,  $k_q$  is a biomolecule quenching rate constant,  $\tau_0$  is an average lifetime of the biomolecule without quencher of  $5 \times 10^{-9}$  s, specifically determined for bovine liver catalase [24],  $[Q]$  is the total concentration of quencher (PCB), and  $K_{SV}$  is SV quenching constant. The obtained slope from SV plot represents  $K_{SV}$ .

A binding constant,  $K_a$ , between catalase and PCB, was determined by applying the following equation [23]:

$$\log \frac{F_0 - F}{F} = -\log \frac{1}{[L] - [P] \frac{F_0 - F}{F_0}} + \log K_a$$

where  $F_0$  and  $F$  are emission signals originating from catalase in the absence and the presence of PCB,  $[L]$  is the total concentration of ligand (PCB), and  $[P]$  is the total concentration of protein (catalase).

For the calculation of thermodynamic parameters of PCB binding to catalase, the same experimental setup and  $K_a$  calculation was performed, but at three temperatures, 25, 30 and 37 °C. The obtained  $K_a$  at three temperatures was used to plot a van't Hoff

graph ( $\ln K_a$  versus  $1/T$ ), from which changes in enthalpy ( $\Delta H$ ) and entropy ( $\Delta S$ ) were calculated using the standard equation:

$$\ln K_a = -\frac{\Delta H}{RT} + \frac{\Delta S}{R}$$

where  $R$  represents the universal gas constant ( $8.314 \text{ J mol}^{-1} \text{ K}^{-1}$ ), and  $T$  is the temperature in kelvins (K). From the graph's slope,  $\Delta H$  was calculated, while  $\Delta S$  was calculated from the intercept. The change in free Gibbs energy ( $\Delta G$ ) was calculated from the equation:

$$\Delta G = \Delta H - T\Delta S$$

Using the same experimental setup, synchronous fluorescence spectra of the catalase/PCB complex were obtained at two different scanning intervals: (i)  $\Delta\lambda = 60 \text{ nm}$ , for the excited Trp residues with emission spectra recorded from 300 to 420 nm, and (ii)  $\Delta\lambda = 15 \text{ nm}$ , for the excited Tyr residues with emission spectra recorded from 290 to 340 nm (where  $\Delta\lambda$  represents a difference between  $\Delta\lambda$  of the emission and the excitation spectra).

The emission spectra of PCB ( $7.85 \mu\text{M}$ ), alone and in the presence of catalase ( $7.85$ ,  $15.7$ , and  $31.4 \mu\text{M}$ ), were also recorded using the same equipment. Phycocyanobilin was excited at  $580 \text{ nm}$ , and emission spectra were recorded in the interval from  $600$  to  $725 \text{ nm}$ . Control spectra, obtained for each tested concentration of catalase, were subtracted from the appropriate spectra obtained in the presence of both catalase and PCB.

### 2.3. Circular dichroism (CD) analysis of catalase/phycocyanobilin complex formation

All CD measurements were performed on a Jasco J-815 spectropolarimeter (JASCO, Japan), under constant nitrogen flow at  $25 \text{ }^\circ\text{C}$ . Far-UV CD spectra of  $7 \mu\text{M}$  catalase in the absence and in the presence of  $7$  and  $14 \mu\text{M}$  PCB were recorded in the range of  $185$ – $260 \text{ nm}$ , using a cell with a  $0.1 \text{ mm}$  path length and with an accumulation of three scans at a scan speed of  $50 \text{ nm/min}$ . The total solution volume was  $60 \mu\text{L}$ . The  $\alpha$ -helical content of protein was determined using two equations [25]:

$$\text{MRE} = \frac{\theta}{10 r l [\text{CAT}]}$$

$$\alpha\text{-helix (\%)} = \frac{-\text{MRE}_{209\text{nm}} - 4000}{29000} \times 100$$

where  $\theta$  is an ellipticity in mdeg at  $209 \text{ nm}$ ,  $r$  is a number of amino acid residues ( $2024$ ),  $l$  is a path length of the cell in  $\text{cm}$  ( $0.01$ ),  $[\text{CAT}]$  is a molar concentration of catalase and MRE is a mean residual ellipticity.

For the near-UV region, the catalase concentration was fixed at  $12 \mu\text{M}$ , while the concentration of PCB in the mixture varied ( $0$ ,  $12$  or  $24 \mu\text{M}$ ) in a total incubation volume of  $1.5 \text{ mL}$ . Spectra were recorded in the range of  $260$ – $320 \text{ nm}$  with an accumulation of two scans at a scan speed of  $100 \text{ nm/min}$ , using a cell of  $10 \text{ mm}$  path length. All CD spectra were baseline corrected by subtracting an appropriate blank spectrum of the solution without catalase.

### 2.4. Determination of thermal stability of catalase/phycocyanobilin complex

The monitoring of catalase thermal denaturation was performed in the temperature range from  $30$  to  $85 \text{ }^\circ\text{C}$ , by increasing temperature at a rate of  $2 \text{ }^\circ\text{C/min}$ . After  $1 \text{ min}$  of equilibration at each temperature, emission spectra were recorded in the range from  $315$  to  $365 \text{ nm}$ , while the excitation wavelength was set to  $280 \text{ nm}$ . Concentrations of catalase and PCB were  $0.5$  and  $5 \mu\text{M}$ , respectively. The results were expressed as the change of the ratio

$F_{350}/F_{330}$  with the temperature (where  $F$  is the emission intensity at a corresponding wavelength) and fitted into a sigmoidal function. The inflection point in the plot was considered as the melting point ( $T_m$ ) of catalase;  $T_m$  is defined as the temperature at which the concentration of the catalase in its folded state equals the concentration of the unfolded protein.

### 2.5. UV-VIS analysis of phycocyanobilin upon binding to catalase

UV-VIS spectra of PCB ( $7.85 \mu\text{M}$ ) alone and in the presence of catalase ( $7.85$ ,  $15.7$ , and  $31.4 \mu\text{M}$ ) were recorded using a UV-1800 spectrophotometer (Shimadzu, Japan). The incubation mixtures were  $2 \text{ mL}$  in volume. Absorbance spectra were recorded in the interval from  $320$  to  $800 \text{ nm}$  using a quartz cuvette with a  $10 \text{ mm}$  path length. All UV-VIS spectra were baseline corrected by subtracting an appropriate blank spectrum of the solution containing only catalase.

### 2.6. Analysis of the catalase activity in the presence of phycocyanobilin

Catalase activity was measured according to a published method [15]. Catalase stock solution was diluted  $125,000$  times and  $10 \mu\text{L}$  of this solution was added to the reaction mixture containing  $12 \text{ mM H}_2\text{O}_2$  in  $20 \text{ mM}$  phosphate buffer in a total reaction volume of  $2 \text{ mL}$ . The activity was measured by following the reduction in absorbance at  $240 \text{ nm}$  for  $2 \text{ min}$  using a UV-1800 spectrophotometer (Shimadzu, Japan). Standardisation of  $\text{H}_2\text{O}_2$  was performed by measuring the absorbance of appropriately diluted  $30\%$  (w/w)  $\text{H}_2\text{O}_2$  (Sigma-Aldrich) at  $240 \text{ nm}$ ; from the obtained absorbance, its concentration was calculated by using an extinction coefficient of  $43.6 \text{ M}^{-1} \text{ cm}^{-1}$  [26]. Catalase activity was measured in the absence and in the presence of PCB at catalase/PCB molar ratios of  $1/10$ ,  $1/100$  and  $1/1000$ . One catalase activity unit (IU) is defined as the amount of enzyme that converts  $1 \mu\text{mol}$  of  $\text{H}_2\text{O}_2$  per minute at  $25 \text{ }^\circ\text{C}$ .

### 2.7. Protection of phycocyanobilin from oxidation in the presence of catalase

Catalase's ability to protect PCB from oxidation was examined using  $2,2'$ -azobis(2-amidinopropane) dihydrochloride (AAPH), a free radical-generating azo compound. The reaction mixture ( $2 \text{ mL}$ ) contained PCB ( $7.85 \mu\text{M}$ ), alone or in the presence of increased concentrations of catalase ( $7.85$ ,  $15.7$ , and  $31.4 \mu\text{M}$ ). After addition of AAPH at a final concentration of  $12 \text{ mM}$ , the resulting solutions were incubated  $40 \text{ min}$  at  $25 \text{ }^\circ\text{C}$ . UV-VIS spectra were then recorded and baseline corrected as described in Section 2.5.

### 2.8. Computational analysis of catalase/phycocyanobilin complex formation

To investigate PCB's interaction with catalase *in silico*, molecular docking using AutoDock Vina (version 1.1.2) was performed [27]. The crystal structure of catalase from bovine liver (PDB code: 1TGU) was obtained from the RCSB Protein Data Bank (<http://www.rcsb.org/>). Because all four bovine liver catalase chains are identical, we selected only chain A for ligand docking. The protonation state of each titratable amino acid was estimated using H++  $3.0$  [28]. Catalase structure was optimised in  $3000$  optimisation steps by CHARMM (version c35b1) [29]. The structure of the PCB ligand in the most stable anionic form was obtained as described [18]. Optimised catalase and PCB were further subjected to Auto Dock Tools (version 1.5.6. Sep\_17\_14) for docking preparation [30]. Ligand single bonds were set to be rotational, while all protein residues were kept rigid. A grid box with the dimensions

$28 \times 28 \times 28 \text{ \AA}$  was used to accommodate the ligand to move freely during a docking simulation. Since the blind docking approach was used to cover the protein's whole volume, a grid box was shifted over the rectangular matrix containing protein with points  $8 \text{ \AA}$  apart. A total of 504 docking runs were made with the exhaustiveness parameter set to 100. From each docking run, nine binding modes with the highest scoring function were kept for analysis.

### 3. Results and discussion

In the presence of increasing PCB concentration, catalase's intrinsic fluorescence was quenched, as shown by spectrofluorimetric analysis (Fig. 1A). From the obtained emission spectra, there was also a blue shift (2 nm) in the emission maximum. Using these spectra, the  $K_a$  of the catalase/PCB complex was calculated to be  $3.9 \times 10^4 \text{ M}^{-1}$  at  $25 \text{ }^\circ\text{C}$  (Fig. 1B). The results suggested one binding site on catalase for PCB ( $n = 0.89$ ). The  $K_a$  of PCB to catalase was similar to that of vitamin C,  $2.3 \times 10^4 \text{ M}^{-1}$  [13], but it was lower than that of resveratrol,  $1.4 \times 10^5 \text{ M}^{-1}$  [14] and quercetin,  $2.2 \times 10^5 \text{ M}^{-1}$  [16]. The Stern-Volmer plot was drawn to demonstrate that static fluorescence quenching (complex formation) was present (Fig. 1C). Since the obtained Stern-Volmer plot was linear ( $r^2 = 0.983$ ; Fig. 1C), it proved that only one type of quenching was present in our tested system. To confirm the quenching type, the SV constant ( $K_{sv}$ ) was calculated from the slope of the obtained SV plot. The  $K_{sv}$  value was found to be  $2.85 \times 10^4 \text{ M}^{-1}$ .

The bimolecular quenching rate constant of  $5.7 \times 10^{12} \text{ M}^{-1} \text{ s}^{-1}$ , calculated from  $K_{sv}$ , was two orders of magnitude higher than the diffusion rate of biomolecules ( $10^{10} \text{ M}^{-1} \text{ s}^{-1}$ ). This confirmed that the intrinsic fluorescence signal quenching of catalase was of static type, rather than a dynamic type. In other words, it was a consequence of complex formation between catalase and PCB.

The calculation of thermodynamic parameters by determination of  $K_a$  at three different temperatures and creation of a van't Hoff graph (Fig. 1D) demonstrated that catalase binding of PCB was driven by enthalpy, as shown by a significant negative value of  $\Delta H$ ,  $-41.9 \text{ kJ mol}^{-1}$ , with a negative value of  $\Delta S$ ,  $-49.7 \text{ J mol}^{-1} \text{ K}^{-1}$ . The change in free Gibbs energy ( $\Delta G$ ) was calculated to be  $-28.2 \text{ kJ mol}^{-1}$ . These results suggested that the binding of PCB to catalase occurred *via* electrostatic interactions and hydrogen bonds [31]. Similar results were obtained for the binding of PCB to human serum albumin [18].

Molecular docking simulation was used to predict the specific binding site of PCB on the catalase A monomer. The enzyme is a tetramer of virtually identical subunits. Each polypeptide chain comprises a helix domain,  $\beta$ -barrel, wrapping domain and threading arm [12]. Docking results revealed that PCB tended to bind between the  $\beta$ -sheet and wrapping domain on catalase monomer. This position is about  $12.5 \text{ \AA}$  from heme, with the docked ligand directed towards the B chain of homotetramer catalase structure and its central cavity (Fig. 2A). No direct interaction was found between PCB and the residues related to enzyme activity (His 61, Asn 133, Phe138, Phe146, conserved Arg339 and unprotonated Tyr343) or the heme group. Instead, the pigment's pyrrole rings

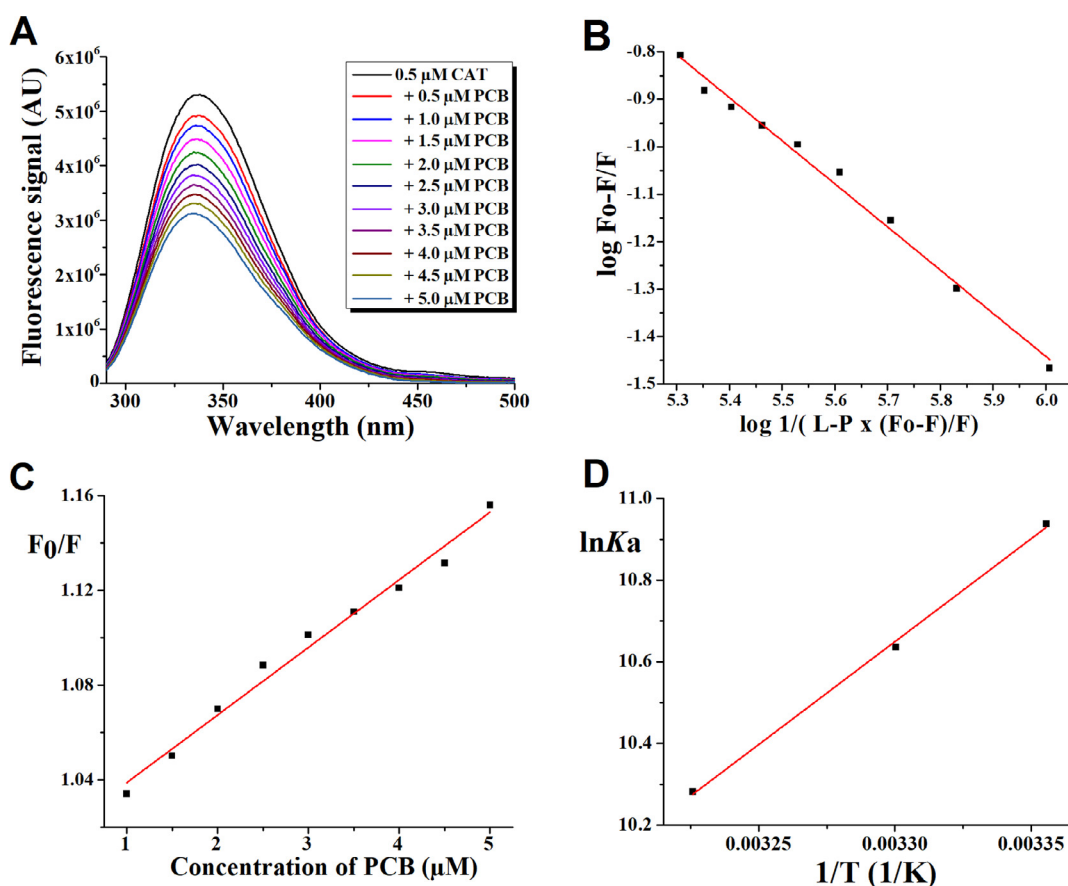


**Fig. 1.** Catalase (CAT) fluorescence quenching by phycocyanobilin (PCB) complex formation and pigment binding characterisation. (A) Emission spectra (excitation at 280 nm) of CAT (0.5 μM) in the presence of increasing PCB concentrations (0–5 μM) at 25 °C, in 20 mM phosphate buffer, pH 7.4. (B) Plot for determination of the binding constant of the CAT/PCB complex at 25 °C. (C) Stern-Volmer plot for the fluorescence quenching of CAT by PCB at 25 °C. (D) van't Hoff plot for the binding constants ( $K_a$ ) at 25, 30, and 37 °C calculated by fluorescence quenching of CAT by PCB.

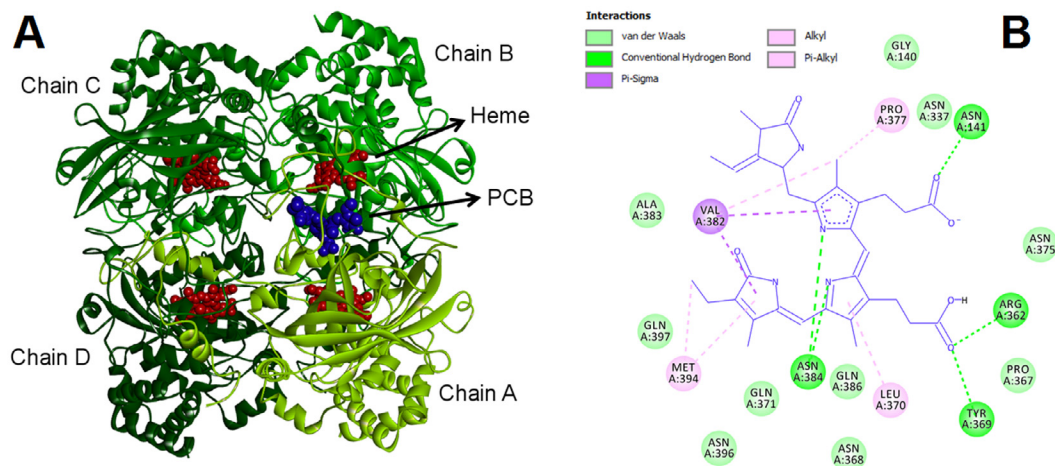


**Fig. 2.** Docking results of the catalase (CAT)/phycocyanobilin (PCB) complex. (A) The binding site of PCB to CAT of lowest energy. (B) Detailed illustration of the interaction pattern between PCB and CAT structural domains, close to the cavity and between the  $\beta$ -barrel and wrapping regions.

formed hydrogen bonds with the amino group of Asn384, and carboxylate anion formed a salt bridge with the amino group of Asn141. In contrast, the carboxyl group of PCB was involved in salt bridge formation with the amino groups of Arg362 and Tyr369. Numerous hydrophobic interactions surrounding amino acid residues (region 360–400 aa) were observed, to further stabilise the complex formation (Fig. 2B). These results were consistent with the results obtained from the fluorescence quenching analysis discussed earlier. The selected binding conformation data indicated that the docking energy score was  $-9.5$  kcal/mol, lower than for pigment binding to human serum albumin [18]. The predicted putative binding site on catalase for PCB was near to those previously reported for bulky ligands, such as resorcinarenes [32] and pioglitazone [33].

Synchronous fluorescence spectra showed that both Trp and Tyr residues were involved in the fluorescence quenching, implying that they were close to the PCB binding pocket on catalase (Fig. 3A and B). An observed small blue shift (2 nm) of emission maximum (Fig. 1A) originated from Trp residues (Fig. 3A), suggesting a change in polarity towards a more hydrophobic environment in the proximity of Trp residues as a consequence of PCB binding.

Far-UV CD spectra were recorded to estimate the effects of PCB binding on secondary structures of catalase. Fig. 3C shows the far-UV spectra of catalase-PCB complex and free protein. The far-UV CD spectrum of catalase contained a broad negative band between 210 and 220 nm, originating from the high content of  $\alpha$ -helix and  $\beta$ -sheet secondary structures in the protein. The shape of the far-UV CD spectra of catalase-PCB complex and of free protein were almost the same, with a minor decrease in negative and positive band intensities occurring upon PCB binding. It was calculated that catalase contained 22.3%  $\alpha$ -helix. In a complex with PCB, the estimated  $\alpha$ -helix content was only slightly decreased, to 20.2%. Therefore, the catalase/PCB complex formation did not alter the secondary structure of the protein significantly.

Near-UV CD spectra of proteins arise from aromatic amino acid side chains. Each aromatic side chain has a characteristic wavelength profile: Trp residues exhibits a peak at about 290 nm, while peaks between 275 and 282 nm arise from Tyr residues [34]. The near-UV CD spectrum of catalase had a characteristic peak at 292 nm, indicating Trp residues' chiral environment. In the catalase/PCB complex spectrum, the peak at 292 nm decreased compared to that of the free protein (Fig. 3D), while a new peak appeared at 285 nm. Therefore, the shapes and amplitudes of spectra indicated that catalase's tertiary structure had changed upon PCB binding, especially near Trp residues.

In aqueous solutions, free PCB does not exhibit optical activity due to an equilibrium between right-hand (*P*) and left-hand (*M*) conformers; *P* stands for PCB conformer with positive (Plus) chirality, while *M* represents conformer with negative (Minus) chirality [18]. Our previous results have shown that peaks appear in the near-UV/VIS CD spectra of PCB upon addition of albumin and preferential binding of only one conformer [18,19]. However, catalase addition did not induce significant changes in PCB's CD spectra (data not shown), indicating no preferential binding of one conformer of PCB over the other to the enzyme.

Denaturation of catalase leads to a redshift of the protein emission peak, allowing the study of its thermal stability and unfolding. Hence, plotting the ratio of fluorescence intensities at 350 and 330 nm against temperature results in a melting curve used to determine the melting point. Melting curves of catalase/PCB complex and free catalase differed significantly (Fig. 3E). The melting curve of the catalase/PCB complex was steeper than the curve of free catalase. Additionally, at lower temperatures, the protein/ligand complex had a smaller  $F_{350}/F_{330}$  ratio than free catalase. These observations can be explained by a blue shift in the catalase emission spectrum due to PCB binding at lower temperatures (Fig. 1A and 3A). Increased temperature caused protein denaturation and dissociation of a protein/ligand complex. Consequently, a steeper increase in the  $F_{350}/F_{330}$  ratio of catalase/PCB complex than free catalase was observed. However, the calculated catalase and catalase/PCB complex's melting temperatures were almost the same (64.2 and 64.7 °C, respectively), indicating that protein thermal stability was not affected by ligand binding. Therefore, the changes in the tertiary structure of catalase did not seem to influence its thermal stability. In agreement with these findings, our previous results have shown an ability of PCB to change the shape of the near-UV CD spectrum of  $\beta$ -lactoglobulin [17], without significant change in its thermal stability.

Although the tertiary structure of catalase changed in the presence of PCB, as demonstrated by the near-UV CD spectra, catalase activity remained almost unaltered (Fig. 3F). No statistical difference ( $p > 0.05$ ; *t*-test) was found between the activities of catalase alone or in the presence of even 1000 times molar excess of PCB. It is worth mentioning that 40% dimethylformamide induced remarkable changes in the near-UV CD spectrum of catalase without influencing its enzyme activity [35]. Each subunit of catalase contains an active site with bound heme *b*; its aggregation into tetramer hides active sites from the solvent [36]. It seemed that the structure of catalase close to its active sites was not significantly altered due to PCB binding. Likewise, PCB itself did not have a sig-

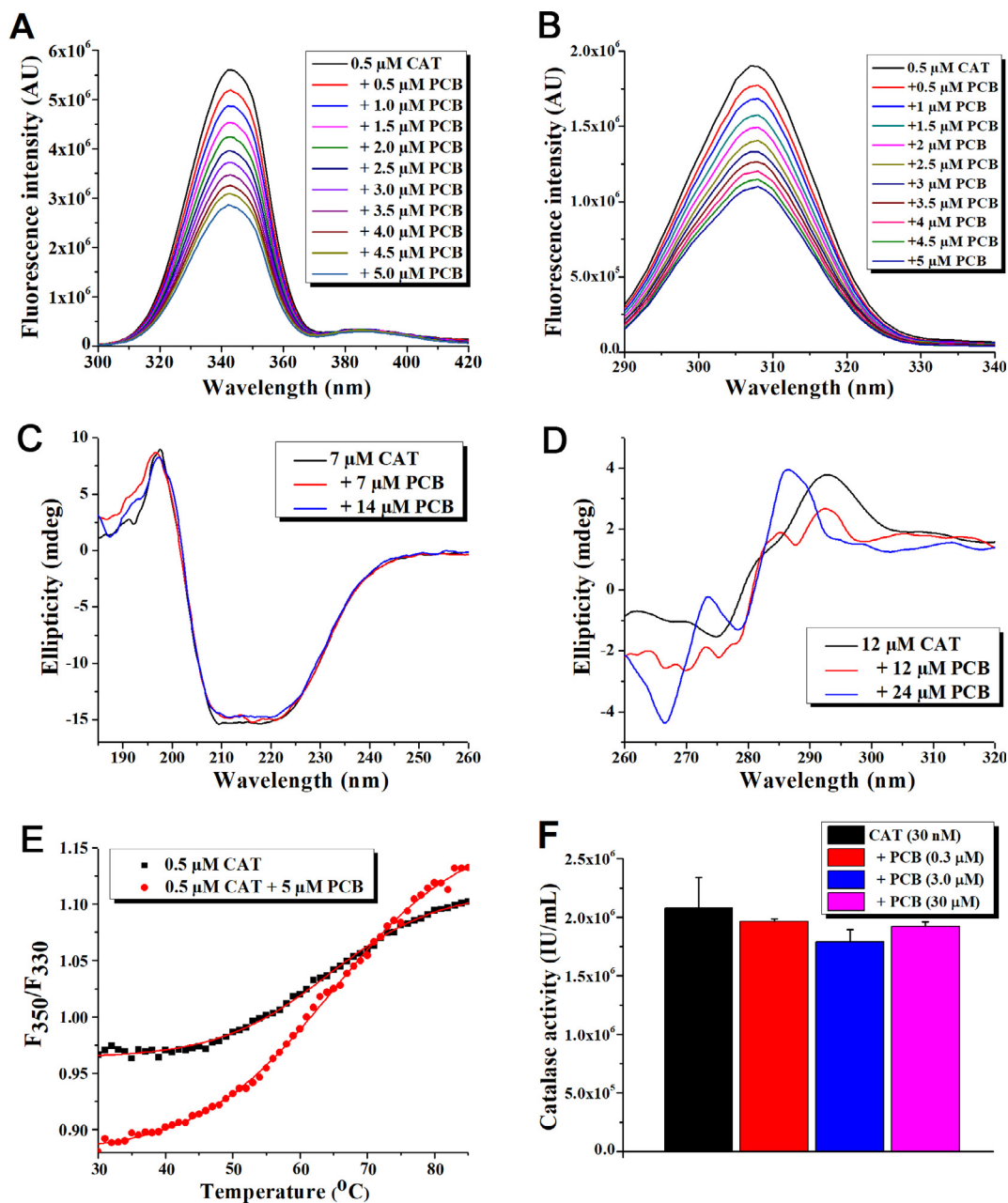


**Fig. 3.** Effects of phycocyanobilin (PCB) complex formation on catalase (CAT) structure and activity. Synchronous fluorescence spectra of CAT with (A)  $\Delta\lambda = 60$  nm (Trp) and with (B)  $\Delta\lambda = 15$  nm (Tyr) in the presence of increasing concentrations of PCB. (C) Far-UV CD spectra of CAT with different concentrations of PCB. (D) Near-UV CD spectra of CAT titrated with varying concentrations of PCB. (E) The change in the ratio of fluorescence intensities at 350 and 330 nm (excitation at 280 nm) with temperature and determination of the melting point (the inflexion point of the curve) of CAT and CAT/PCB complex (in molar ratio 1:10). (F) CAT activity (IU/mL) in the absence and presence of different concentrations of PCB; data were pooled from three independent experiments, and error bars indicate SD. All experiments were performed at 25 °C, in 20 mM phosphate buffer, pH 7.4.

nificant effect on catalase activity upon binding. Similar results were obtained for aspirin binding to catalase. Even though aspirin caused considerable alteration of the catalase structure, no alteration in the enzyme activity was detected [37]. On the other hand, some ligands (such as ellagic acid) may increase the activity of catalase [38], whereas others (such as resorcinarenes) may decrease it [32].

PCB can be excited at 580 nm to emit at a maximum of 640 nm. In the presence of increased catalase concentration, the intensity of the emission maximum of PCB declined, as shown in Fig. 4A. One possible explanation for this finding can be the Förster resonance energy transfer (FRET) effect [39]. This effect is present when the

acceptor's absorption spectrum (in this case, the heme in catalase has a small absorption peak at 625 nm) overlaps with the donor's emission spectrum (PCB at 640 nm), suggesting possible dipole-dipole interactions between heme and PCB. This observation is another indication that pigment PCB bound to catalase.

The UV-VIS spectra of PCB in the presence of catalase at varying concentrations were almost unaltered (Fig. 4B), in contrast to the bovine serum albumin/PCB complex [19]. This result indicated that PCB binding to catalase did not influence conformation, polarity, or protonation state of the pigment, which could be monitored to reduce the absorption intensity or a blue/redshift of its absorption maximum [18,19]. In contrast to these findings, a blue shift was

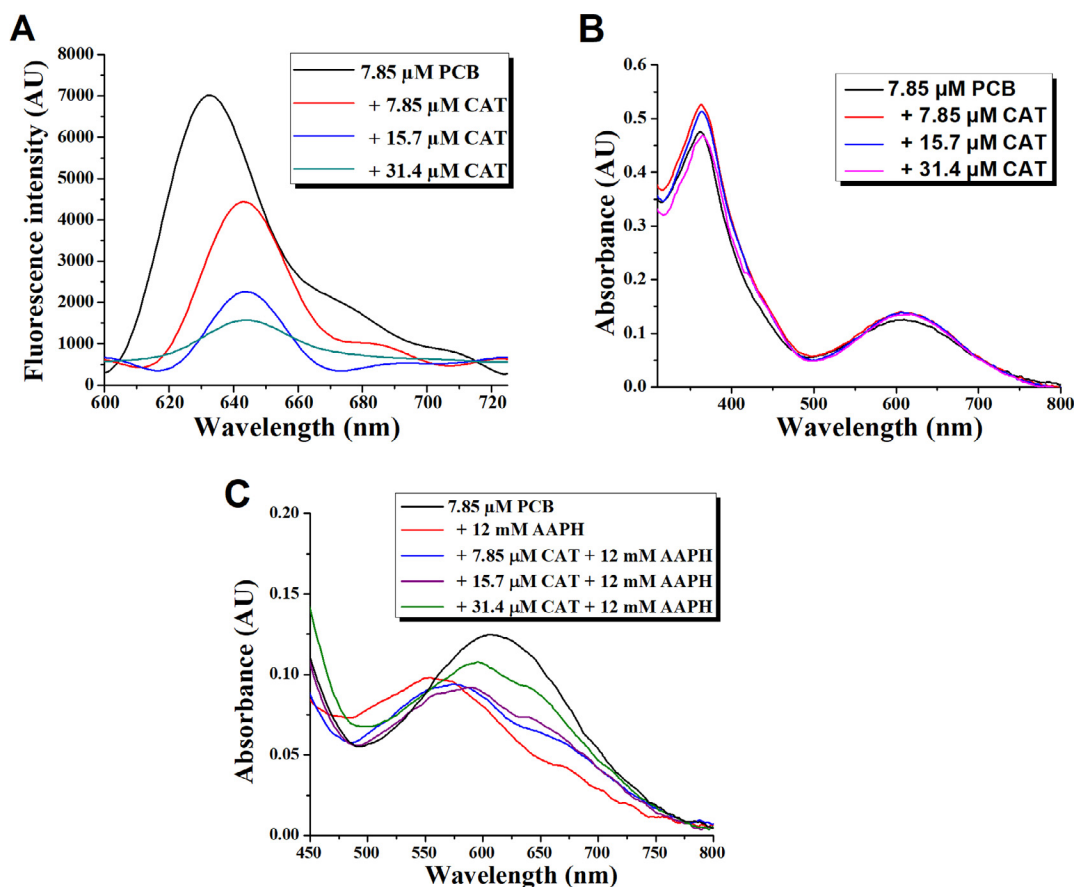


**Fig. 4.** Effects of catalase (CAT)/phycocyanobilin (PCB) complex formation on pigment properties. (A) Emission (excitation at 580 nm) and (B) UV–VIS spectra of PCB in the presence of different concentrations of CAT. (C) VIS spectra of PCB, alone or in the presence of a fixed concentration of free-radical generator 2,2′-azobis (2-amidinopropane) dihydrochloride (AAPH) and varying CAT concentrations. All experiments were performed at 25 °C, in 20 mM phosphate buffer, pH 7.4.

observed on PCB's high-affinity binding to human serum albumin [40].

The absence of stereoselective pigment binding, the modest association constant without changes in ligand conformation, together with the predicted interactions pattern, all point to the conclusion that the binding site(s) for PCB on catalase tetramer was loosely structured.

Incubation of PCB with AAPH, an oxygen-free radical generator, for 40 min at 25 °C resulted in a reduction of PCB absorption in the visible part of its spectrum with a significant blueshift of its absorption maximum. Blueshift decreases with increasing catalase concentrations, while the absorption intensity is closer to nonmodified PCB (Fig. 4C). These results suggest that catalase could bind PCB and protect it from oxidation, thus prolonging its bioactivity. A plausible explanation for this phenomenon was that catalase directly scavenges peroxy radicals formed by the decomposition of AAPH in aqueous solutions [13,41].

On the other hand, as various reactive oxygen species (ROS) can inhibit catalase [42], their scavenging by the bound PCB could diminish ROS-induced inhibition of an enzyme [43]. It is worth mentioning that PCB is not only a potent antioxidant [44], but it can also induce an innate antioxidant mechanism. For example, PCB was shown to activate atheroprotective heme oxygenase in endothelial cells, which is considered an essential mechanism for reducing atherosclerosis [45]. Furthermore, potent anti-cancer and immunomodulatory effects of PCB [46] are ascribed to its antioxidant and radical scavenging properties [43].

The exact mechanisms behind PCB and/or PCB-carrying peptides transport from the gastrointestinal tract to the circulation

are currently unknown [3]. Preservation of PCB in its active state, for example, by binding to different proteins is crucial for exerting its health-promoting effects. As already mentioned, human serum albumin can bind PCB with high affinity and serve as its protective carrier in the circulation [18,40]. Catalase can serve this purpose by binding PCB with moderate affinity and concentrating it in erythrocytes. An *in vitro* study previously demonstrated that C-PC could protect the erythrocyte membrane from oxidative damage [47]. Phycocyanobilin is most likely responsible for this effect as C-PC's health benefits most likely arise from the attached PCB. To date there are no concentrated PCB formulations in clinical treatments or as food supplements [48]. Manufacturing PCB formulations or PCB-enriched *Spirulina* powders could prove beneficial for human health, notably in conditions characterised by increased oxidative stress.

#### 4. Conclusion

The interaction between bovine liver catalase and nutraceutical PCB was investigated using different spectroscopic techniques complemented with a molecular docking study. Catalase's microenvironment and conformation were altered due to PCB binding, as seen from fluorescence, synchronous fluorescence and near-UV CD spectra. However, no profound structural change of catalase occurred in the pigment's presence, as revealed by far-UV CD studies. The same was true for enzyme activity in the presence of pigment – it remained unaffected. Molecular docking simulations demonstrated that PCB most likely bound to amino acid residues from the  $\beta$ -barrel and wrapping domain, near the central

cavity of catalase. These results supplemented the wet laboratory experimental results. The relationship between catalase and PCB is, on the other hand, beneficial for PCB as catalase effectively reduces free-radical induced pigment oxidation. This effect may translate *in vivo* and provide health benefits.

### CRedit authorship contribution statement

**Nikola Gligorijević:** Methodology, Investigation, Formal analysis, Writing - original draft, Data curation. **Simeon Minić:** Conceptualization, Methodology, Investigation, Formal analysis, Writing - original draft. **Milica Radibratović:** Methodology, Investigation, Formal analysis, Writing - original draft. **Vassiliki Papadimitriou:** Formal analysis, Writing - review & editing. **Olgica Nedić:** Writing - review & editing, Funding acquisition. **Theodore G. Sotiroudis:** Conceptualization, Supervision, Writing - review & editing. **Milan R. Nikolić:** Conceptualization, Investigation, Formal analysis, Resources, Writing - review & editing, Funding acquisition.

### Declaration of Competing Interest

The authors declare that they have no known competing financial interests or personal relationships that could have appeared to influence the work reported in this paper.

### Acknowledgement

This work was supported by the Ministry of Education, Science and Technological Development of the Republic of Serbia (Contract number: 451-03-68/2020-14/200168). The authors thank Dr David R. Jones for language editing and proof-reading the manuscript.

### References

- [1] Q. Liu, Y. Huang, R. Zhang, T. Cai, Y. Cai, Medical application of spirulina platensis derived C-phycoerythrin, Evidence-Based Complement Altern. Med. 2016 (2016) 7803846, <https://doi.org/10.1155/2016/7803846>.
- [2] T. Watermann, H. Elgabarty, D. Sebastiani, Phycocyanobilin in solution-a solvent triggered molecular switch, Phys. Chem. Chem. Phys. 16 (2014) 6146–6152, <https://doi.org/10.1039/c3cp54307b>.
- [3] D. Stanic-Vucinic, S. Minić, M.R. Nikolic, T. Cirkovic Velickovic, Spirulina Phycobiliproteins as Food Components and Complements, In: E. Jacob-Lopes (Ed.), Microalgal Biotechnol., First Edition, IntechOpen, Rijeka, 2018, pp. 129–149, doi: 10.5772/intechopen.73791.
- [4] M. Kuddus, P. Singh, G. Thomas, A. Al-Hazimi, Recent developments in production and biotechnological applications of C-phycoerythrin, Biomed Res. Int. 2013 (2013), <https://doi.org/10.1155/2013/742859>.
- [5] N.T. Eriksen, Production of phycocyanin - a pigment with applications in biology, biotechnology, foods and medicine, Appl. Microbiol. Biotechnol. 80 (2008) 1–14, <https://doi.org/10.1007/s00253-008-1542-y>.
- [6] A.N. Glazer, Phycobiliproteins - a family of valuable, widely used fluorophores, J. Appl. Phycol. 6 (1994) 105–112, <https://doi.org/10.1007/BF02186064>.
- [7] J. Marín-Prida, N. Pavón-Fuentes, A. Llópiz-Arzuaga, J.R. Fernández-Massó, L. Delgado-Roche, Y. Mendoza-Marí, S.P. Santana, A. Cruz-Ramírez, C. Valenzuela-Silva, M. Nazábal-Gálvez, A. Cintado-Benítez, G.L. Pardo-Andreu, N. Polentarutti, F. Riva, E. Pentón-Arias, G. Pentón-Rol, Phycocyanobilin promotes PC12 cell survival and modulates immune and inflammatory genes and oxidative stress markers in acute cerebral hypoperfusion in rats, Toxicol. Appl. Pharmacol. 272 (2013) 49–60, <https://doi.org/10.1016/j.taap.2013.05.021>.
- [8] M. Cervantes-Llanos, N. Lagumersindez-Denis, J. Marín-Prida, N. Pavón-Fuentes, V. Falcon-Cama, B. Piniella-Matamoros, H. Camacho-Rodríguez, J.R. Fernández-Massó, C. Valenzuela-Silva, I. Raíces-Cruz, E. Pentón-Arias, M.M. Teixeira, G. Pentón-Rol, Beneficial effects of oral administration of C-Phycocyanin and Phycocyanobilin in rodent models of experimental autoimmune encephalomyelitis, Life Sci. 194 (2018) 130–138, <https://doi.org/10.1016/j.lfs.2017.12.032>.
- [9] J. Zheng, T. Inoguchi, S. Sasaki, Y. Maeda, M.F. McCarty, M. Fujii, N. Ikeda, K. Kobayashi, N. Sonoda, R. Takayanagi, Phycocyanin and phycocyanobilin from Spirulina platensis protect against diabetic nephropathy by inhibiting oxidative stress, Am. J. Physiol. Regul. Integr. Comp. Physiol. 304 (2013) R110–R120, <https://doi.org/10.1152/ajpregu.00648.2011>.
- [10] G. Pentón-Rol, J. Marín-Prida, V. Falcón-Cama, C-phycoerythrin and phycocyanobilin as remyelination therapies for enhancing recovery in multiple sclerosis and ischemic stroke: a preclinical perspective, Behav. Sci. (Basel) 8 (2018) 15, <https://doi.org/10.3390/bs8010015>.
- [11] H. Sies, Hydrogen peroxide as a central redox signaling molecule in physiological oxidative stress: oxidative eustress, Redox Biol. 11 (2017) 613–619, <https://doi.org/10.1016/j.redox.2016.12.035>.
- [12] C. Glorieux, P.B. Calderon, Catalase, a remarkable enzyme: Targeting the oldest antioxidant enzyme to find a new cancer treatment approach, Biol. Chem. 398 (2017) 1095–1108, <https://doi.org/10.1515/hsz-2017-0131>.
- [13] D. Li, B. Ji, J. Jin, Spectrophotometric studies on the binding of Vitamin C to lysozyme and bovine liver catalase, J. Lumin. 128 (2008) 1399–1406, <https://doi.org/10.1016/j.jlumin.2008.01.010>.
- [14] S. Rashtbari, G. Dehghan, R. Yekta, A. Jouyban, M. Iranshahi, Effects of resveratrol on the structure and catalytic function of bovine liver catalase (BLC): spectroscopic and theoretical studies, Adv. Pharm. Bull. 7 (2017) 349–357, <https://doi.org/10.15171/apb.2017.042>.
- [15] F.M. Najjar, R. Ghadiri, R. Yousefi, N. Safari, V. Sheikhasani, N. Sheibani, A.A. Moosavi-Movahedi, Studies to reveal the nature of interactions between catalase and curcumin using computational methods and optical techniques, Int. J. Biol. Macromol. 95 (2017) 550–556, <https://doi.org/10.1016/j.ijbiomac.2016.11.050>.
- [16] S. Rashtbari, G. Dehghan, R. Yekta, A. Jouyban, Investigation of the binding mechanism and inhibition of bovine liver catalase by quercetin: multi-spectroscopic and computational study, BiolImpacts. 7 (2017) 147–153, <https://doi.org/10.15171/bi.2017.18>.
- [17] S. Minić, M. Radomirovic, N. Savkovic, M. Radibratovic, J. Mihailovic, T. Vasovic, M. Nikolic, M. Milcic, D. Stanic-Vucinic, T. Cirkovic Velickovic, Covalent binding of food-derived blue pigment phycocyanobilin to bovine  $\beta$ -lactoglobulin under physiological conditions, Food Chem. 269 (2018) 43–52, <https://doi.org/10.1016/j.foodchem.2018.06.138>.
- [18] S.L. Minić, M. Milcic, D. Stanic-Vucinic, M. Radibratovic, T.G. Sotiroudis, M.R. Nikolic, T.C. Velickovic, Phycocyanobilin, a bioactive tetrapyrrolic compound of blue-green alga Spirulina, binds with high affinity and competes with bilirubin for binding on human serum albumin, RSC Adv. 5 (2015) 61787–61798, <https://doi.org/10.1039/c5ra05534b>.
- [19] S. Minić, D. Stanic-Vucinic, M. Radomirovic, M. Radibratovic, M. Milcic, M. Nikolic, T. Cirkovic Velickovic, Characterization and effects of binding of food-derived bioactive phycocyanobilin to bovine serum albumin, Food Chem. 239 (2018) 1090–1099, <https://doi.org/10.1016/j.foodchem.2017.07.066>.
- [20] E. Fu, L. Friedman, H.W. Siegelman, Mass-spectral identification and purification of phycoerythrobilin and phycocyanobilin, Biochem. J. 179 (1979) 1–6, <https://doi.org/10.1042/bj1790001>.
- [21] W.J. Cole, D.J. Chapman, H.W. Siegelman, The structure of phycocyanobilin, J. Am. Chem. Soc. 89 (1967) 3643–3645, <https://doi.org/10.1021/ja00990a054>.
- [22] T.T. Herskovits, Solvent perturbation studies colored of heme proteins, Arch. Biochem. Biophys. 130 (1969) 19–29, [https://doi.org/10.1016/0003-9861\(69\)90004-6](https://doi.org/10.1016/0003-9861(69)90004-6).
- [23] J.R. Lakowicz, Principles of Fluorescence Spectroscopy, third ed., Springer US, New York, 2006. doi: 10.1007/978-0-387-46312-4.
- [24] Y. Yang, D. Li, Investigation on the interaction between isorhamnetin and bovine liver catalase by spectroscopic techniques under different pH conditions, Luminescence 31 (2016) 1130–1137, <https://doi.org/10.1002/bio.3082>.
- [25] I. Matei, M. Hillebrand, Interaction of kaempferol with human serum albumin: a fluorescence and circular dichroism study, J. Pharm. Biomed. Anal. 51 (2010) 768–773, <https://doi.org/10.1016/j.jpba.2009.09.037>.
- [26] A.G. Hildebrandt, I. Roots, Reduced nicotinamide adenine dinucleotide phosphate (NADPH)-dependent formation and breakdown of hydrogen peroxide during mixed function oxidation reactions in liver microsomes, Arch. Biochem. Biophys. 171 (1975) 385–397, [https://doi.org/10.1016/0003-9861\(75\)90047-8](https://doi.org/10.1016/0003-9861(75)90047-8).
- [27] O. Trott, A.J. Olson, AutoDock Vina: improving the speed and accuracy of docking with a new scoring function, efficient optimization, and multithreading, J. Comput. Chem. 31 (2010) 455–461, <https://doi.org/10.1002/jcc.21334>.
- [28] J.C. Gordon, J.B. Myers, T. Folta, V. Shoja, L.S. Heath, A. Onufriev, H++: a server for estimating pKas and adding missing hydrogens to macromolecules, Nucleic Acids Res. 33(Web Server issue) (2005) W368–W371, doi: 10.1093/nar/gki464.
- [29] A.D. MacKerell Jr., D. Bashford, M. Bellott, R.L. Dunbrack Jr., J.D. Evanseck, M.J. Field, S. Fischer, J. Gao, H. Guo, S. Ha, D. Joseph-McCarthy, L. Kuchnir, K. Kuczyra, F.T.K. Lau, C. Mattos, S. Michnick, T. Ngo, D.T. Nguyen, B. Prodhom, W. E. Reiher, B. Roux, M. Schlenkrich, J.C. Smith, R. Stote, J. Straub, M. Watanabe, J. Wiórkiewicz-Kuczera, D. Yin, M. Karplus, All-atom empirical potential for molecular modeling and dynamics studies of proteins, J. Phys. Chem. B. 102 (1998) 3586–3616, <https://doi.org/10.1021/jp973084f>.
- [30] G.M. Morris, R. Huey, W. Lindstrom, M.F. Sanner, R.K. Belew, D.S. Goodsell, A.J. Olson, AutoDock4 and AutoDockTools4: automated docking with selective receptor flexibility, J. Comput. Chem. 30 (2009) 2785–2791, <https://doi.org/10.1002/jcc.21256>.
- [31] P.D. Ross, S. Subramanian, Thermodynamics of protein association reactions: forces contributing to stability, Biochemistry. 20 (1981) 3096–3102, <https://doi.org/10.1021/bi00514a017>.
- [32] N. Collazos, G. García, A. Malagón, O. Caicedo, E.F. Vargas, Binding interactions of a series of sulfonated water-soluble resorcinarenes with bovine liver catalase, Int. J. Biol. Macromol. 139 (2019) 75–84, <https://doi.org/10.1016/j.ijbiomac.2019.07.197>.

- [33] R. Yekta, G. Dehghan, S. Rashtbari, N. Sheibani, A.A. Moosavi-Movahedi, Activation of catalase by pioglitazone: multiple spectroscopic methods combined with molecular docking studies, *J. Mol. Recognit.* 30 (2017), <https://doi.org/10.1002/jmr.2648>.
- [34] S. Kelly, N. Price, The use of circular dichroism in the investigation of protein structure and function, *Curr. Protein Pept. Sci.* 1 (2000) 349–384, <https://doi.org/10.2174/1389203003381315>.
- [35] M. Rehan, H. Younus, Effect of organic solvents on the conformation and interaction of catalase and anticatalase antibodies, *Int. J. Biol. Macromol.* 38 (2006) 289–295, <https://doi.org/10.1016/j.ijbiomac.2006.03.023>.
- [36] C.D. Putnam, A.S. Arvai, Y. Bourne, J.A. Tainer, Active and inhibited human catalase structures: ligand and NADPH binding and catalytic mechanism, *J. Mol. Biol.* 296 (2000) 295–309, <https://doi.org/10.1006/jmbi.1999.3458>.
- [37] B. Koohshekan, A. Divsalar, M. Saiedifar, A.A. Saboury, B. Ghalandari, A. Gholamian, A. Seyedarabi, Protective effects of aspirin on the function of bovine liver catalase: a spectroscopy and molecular docking study, *J. Mol. Liq.* 218 (2016) 8–15, <https://doi.org/10.1016/j.molliq.2016.02.022>.
- [38] S. Rashtbari, S. Khataee, M. Iranshahi, A.A. Moosavi-Movahedi, G. Hosseinzadeh, G. Dehghan, Experimental investigation and molecular dynamics simulation of the binding of ellagic acid to bovine liver catalase: activation study and interaction mechanism, *Int. J. Biol. Macromol.* 143 (2020) 850–861, <https://doi.org/10.1016/j.ijbiomac.2019.09.146>.
- [39] R. Sridharan, J. Zuber, S.M. Connelly, E. Mathew, M.E. Dumont, Fluorescent approaches for understanding interactions of ligands with G protein coupled receptors, *Biochim. Biophys. Acta - Biomembr.* 2014 (1838) 15–33, <https://doi.org/10.1016/j.bbamem.2013.09.005>.
- [40] M. Radibratovic, S. Minic, D. Stanic-Vucinic, M. Nikolic, M. Milcic, T.C. Velickovic, Stabilization of human serum albumin by the binding of phycocyanobilin, a bioactive chromophore of blue-green alga spirulina: molecular dynamics and experimental study, *PLoS One.* 11 (2016), <https://doi.org/10.1371/journal.pone.0167973> e0167973.
- [41] M.C. Krishna, M.W. Dewhirst, H.S. Friedman, J.A. Cook, W. DeGraff, A. Samuni, A. Russo, J.B. Mitchell, Hyperthermic sensitization by the radical initiator 2,2'-azobis (2-amidinopropane) dihydrochloride (AAPH). I. *In vitro* studies, *Int. J. Hyperthermia.* 10 (1994) 271–281, <https://doi.org/10.3109/02656739409009348>.
- [42] L. Gebicka, J. Krych-Madej, The role of catalases in the prevention/promotion of oxidative stress, *J. Inorg. Biochem.* 197 (2019), <https://doi.org/10.1016/j.jinorgbio.2019.110699> 110699.
- [43] C. Romay, R. González, N. Ledón, D. Ramirez, V. Rimbau, C-phycocyanin: a biliprotein with antioxidant, anti-inflammatory and neuroprotective effects, *Curr. Protein Pept. Sci.* 4 (2003) 207–216, <https://doi.org/10.2174/1389203033487216>.
- [44] T. Hirata, M. Tanaka, M. Ooike, T. Tsunomura, M. Sakaguchi, Antioxidant activities of phycocyanobilin prepared from *Spirulina platensis*, *J. Appl. Phycol.* 12 (2000) 435–439, <https://doi.org/10.1023/A:1008175217194>.
- [45] Z. Strasky, L. Zemankova, I. Nemeckova, J. Rathouska, R.J. Wong, L. Muchova, I. Subhanova, J. Vanikova, K. Vanova, L. Vitek, P. Nachtigal, *Spirulina platensis* and phycocyanobilin activate atheroprotective heme oxygenase-1: a possible implication for atherogenesis, *Food Funct.* 4 (2013) 1586–1594, <https://doi.org/10.1039/c3fo60230c>.
- [46] M.F. McCarty, Clinical potential of phycocyanobilin for induction of T regulatory cells in the management of inflammatory disorders, *Med. Hypotheses.* 77 (2011) 1031–1033, <https://doi.org/10.1016/j.mehy.2011.08.041>.
- [47] C. Romay, R. Gonzalez, Phycocyanin is an antioxidant protector of human erythrocytes against lysis by peroxy radicals, *J. Pharm. Pharmacol.* 52 (2000) 367–368, <https://doi.org/10.1211/0022357001774093>.
- [48] M.F. McCarty, Supplementation with phycocyanobilin, citrulline, taurine, and supranutritional doses of folic acid and biotin-potential for preventing or slowing the progression of diabetic complications, *Healthcare.* 5 (2017) 15, <https://doi.org/10.3390/healthcare5010015>.